Published in final edited form as:
Biochemistry. 2012 December 4; 51(48): 9595–9602. doi:10.1021/bi301413y.

Metamorphic Protein IscU Changes Conformation by *cis-trans* Isomerizations of Two Peptidyl-Prolyl Peptide Bonds[†]

Ziqi Dai[‡], **Marco Tonelli**[§], and **John L. Markley**[*,§]
Graduate Program in Biophysics, National Magnetic Resonance Facility at Madison and Department of Biochemistry, University of Wisconsin–Madison, Madison, Wisconsin 53706, USA

Abstract

IscU from *Escherichia coli*, the scaffold protein for iron-sulfur cluster biosynthesis and transfer, populates two conformational states with similar free energies and with lifetimes on the order of one second that interconvert in an apparent two-state reaction. One state (S) is structured, and the other (D) is largely disordered, but both play essential functional roles. We report here NMR studies demonstrating that all four prolyl residues of apo-IscU (P14, P35, P100, and P101) are *trans* in the S-state but that two absolutely conserved residues (P14, P101) become *cis* in the D-state. The peptidyl-prolyl peptide bond configurations were determined by analyzing assigned chemical shifts and were confirmed by measurements of nuclear Overhauser effects. We conclude that the S⇄D interconversion involves concerted *trans-cis* isomerization of the N13–P14 and P100–P101 peptide bonds. Although the D-state is largely disordered, we show that it contains an ordered domain that accounts for the stabilization of two high-energy *cis* peptide bonds. Thus, IscU may be classified as a metamorphic protein.

Keywords

conformational change; iron-sulfur cluster assembly and transfer; metamorphic protein; NMR spectroscopy; order-disorder conversion; peptidyl-prolyl peptide bond configuration; protein sequence conservation; stable isotope labeling

Iron-sulfur (Fe-S) cluster proteins are central to many cellular activities including nitrogen fixation, metabolic catalysis, regulation of gene expression, and electron transfer (1–3). The machinery that generates Fe-S clusters is highly conserved across all species. Bacteria can contain three Fe-S cluster assembly systems: Nif (nitrogen fixation), Isc (iron sulfur cluster), and Suf (sulfur formation). Of these, the Isc system is responsible for assembling and delivering clusters for most iron-sulfur proteins in bacteria and also is operational in the mitochondria of eukaryotes (1). Defects in the Isc machinery underlie aging processes and a number of human diseases (4–7). IscU (Isu1 and Isu2 in yeast, ISCU in human) is the scaffold protein on which the iron-sulfur cluster is assembled and delivered to receiver apo-

[†]This work was supported by US National Institutes of Health (NIH) grants R01 GM58667 and U01 GM94622 in collaboration with the National Magnetic Resonance Facility at Madison which is supported by NIH grants from the National Center for Research Resources (5P41RR002301-27 and RR02301-26S1) and the National Institute for General Medical Sciences (8P41 GM103399-27).

[*]To whom correspondence should be addressed. Telephone: (608) 263-9349; markley@nmrfam.wisc.edu.
[‡]Biophysics Graduate Program
[§]National Magnetic Resonance Facility at Madison and Department of Biochemistry

SUPPORTING INFORMATION AVAILABLE
Alignment of sequences of IscU proteins illustrating their conservation (Figure S1); NMR spectra from Figure 1 plotted at a lower contour (Figure S2); representations of *trans* and *cis* peptidyl–prolyl peptide bonds illustrating expected NOEs (Figure S3). This material is available free of charge via the Internet at http://pubs.acs.org.

proteins. IscU interacts with most of the other proteins in the Isc pathway, including the cysteine desulfurase that donates sulfur (8–11) and the specialized DnaK/DnaJ-type co-chaperone pair that facilitates cluster transfer *in vivo* in an ATP-dependent mechanism (12–14).

IscU from *Escherichia coli* populates two interconverting conformational states: one state (S) is structured and has yielded an NMR structure (PDB 2L4X) (15), and the other (D) is dynamically disordered and lacks the secondary structural elements found in the S-state (16, 17). At pH 8.0 and 25 °C, the S→D rate is 0.77 s^{-1} and the D→S rate is 2.0 s^{-1} (17). Both states have been shown to be functionally essential in that the D-state is the substrate for the cysteine desulfurase IscS (17) and is the form present in the HscA:IscU complex (18), whereas the S-state binds preferentially to the DnaJ-type co-chaperone HscB (16, 18) and also is the conformational state of the protein when it contains a [2Fe-2S] cluster (19). Because residues observed by NMR spectroscopy exhibit two separate peaks corresponding to the S and D states (16, 17), the interconversion appears to be two-state.

We suspected that a peptidyl-prolyl *cis*/*trans* isomerization might account for the slow step in the interconversion. We report here NMR studies showing that all four prolyl residues of apo-IscU (P14, P35, P100, and P101) are *trans* in the S-state, but that two (P14, P101) become *cis* in the D-state. The two prolyl residues involved are strictly conserved in the sequences of all IscU proteins (see Figure S1 available online). Proline at residues 101 has been shown to be essential for recognition by the Hsp70-type chaperone HscA (20), and substitution of the homologous proline for alanine in yeast Isu led to a slow growth phenotype (21). These results imply that the D-state, which supports two high-energy *cis* peptide bonds, cannot be fully disordered. This expectation is confirmed by NOE results that show that the D-state contains ordered and disordered domains. We conclude that IscU has evolved to interconvert between two conformational states that serve different functions in the cycle of iron-sulfur cluster assembly and delivery.

EXPERIMENTAL PROCEDURES

Protein production and purification

Labeled amino acids were purchased from Cambridge Isotope Laboratories (Andover, MA). [U-^{13}C, ^{15}N-Pro]-IscU and [U-^{13}C,^{15}N-Pro, U-^{15}N-Ala]-IscU were prepared according to a modification of a published procedure (22). A colony of BL21 cells transformed with the pTrc 99A plasmid containing IscU gene was used to inoculate 5 ml of TB liquid medium containing 100 μg/ml ampicillin. The cells were grown overnight at 37 °C, and a 100 μl aliquot was used to inoculate 250 ml of TB liquid medium containing 100 μg/ml ampicillin. This culture was grown for 12 h at 37 °C. Cells isolated from this 250 ml culture by centrifugation were used to inoculate 1000 ml of M9 medium containing 100 μg/ml ampicillin and supplemented with 1 ml of vitamin solution (22), 1 g of NH_4Cl and 4 g of glucose and a cocktail containing the labeled amino acids to be incorporated along with unlabeled amino acids (23). [U-^{13}C, U-^{15}N]-IscU was prepared in a similar fashion, except that the medium contained 1 g of [U-^{15}N]-NH_4Cl, and 3 g [U-^{13}C]-glucose and no labeled amino acids. The culture was induced when $OD_{600}\approx1$ by adding IPTG to a final concentration of 0.4 mM. Protein was purified as described previously (22, 24). The elution buffer consisted of 50 mM Tris-HCl (pH 8.0), 1 mM DTT, 0.5 mM EDTA, and 150 mM NaCl. Fractions were analyzed by gel electrophoresis, and those appearing homogeneous were pooled, concentrated by ultrafiltration, frozen in liquid nitrogen, and stored at −80 °C. The isotopic labeling efficiency as determined by mass spectrometry was ~92%. Zn^{2+}-bound IscU was prepared by gradually adding aliquots from a stock buffer containing 50 mM Tris-HCl (pH 8.0), 10 mM $ZnCl_2$, and 150 mM NaCl to a solution of apo-IscU.

NMR spectroscopy and data analysis

DSS was used as an internal reference for all NMR chemical shift measurements. NMR data were collected at the National Magnetic Resonance Facility at Madison (NMRFAM) on Varian VNMRS spectrometers equipped with *z*-gradient cryogenic probes. NMRPipe (25) was used to process the raw NMR data. SPARKY (26) was used for data analysis. The resonance assignments of apo-IscU were based in part on previous results (16, 17).

Data Deposition

Assigned chemical shifts acquired at 45 °C and 25 °C in the presence of Zn^{2+} have been deposited at BMRB under accession codes 18754 and 18750, respectively.

RESULTS

Proline NMR peak assignments

The two-dimensional (2D) ^{1}H-^{13}C HSQC NMR spectrum of [U-^{13}C, ^{15}N-Pro]-IscU (IscU produced biosynthetically with incorporation of proline labeled with the stable isotopes ^{13}C and 15N) collected at pH 8.0 and 25 °C, where both the S- and D-states are populated at a [S]/[D] ratio of ~2.6, revealed a single set of peaks for P35, two sets of peaks for P100 and P101, and three sets of peaks for P14 (Figure 1a). To observe peaks from the S-state alone, we added Zn^{2+}, which constrains the protein to the S-state (17), and collected data at 25 °C (Figure 1b). To observe peaks from the D-state alone, we took advantage of the temperature dependence of the S⇄D equilibrium, which shifts toward the D-state at higher temperatures so that at 45 °C only signals from the D-state were observed (Figure 1c). Plots of the same data at lower contour levels did not reveal any additional signals from prolyl residues (Figure S2).

To assign signals to the four individual prolyl residues, we prepared a selectively labeled sample of IscU by biosynthetic incorporation of [U-^{13}C, ^{15}N]-Pro and [^{15}N]-Ala. This labeling pattern enabled us to identify the spin system of P35 from the P35$^{13}C^{\alpha}$-A36^{15}N connectivity, the spin systems of P100 and P101 from the P100$^{13}C^{\alpha}$-P101^{15}N connectivity, and the spin system of P14 by exclusion. To identify these connectivities in the S-state, we collected a three-dimensional (3D) HACAN spectrum (27) of the Zn^{2+} complex, which allowed the observation of signals from $^{1}H^{\alpha}$-$^{13}C^{\alpha}$ of residue *i* to its own nitrogen ($^{1}H^{\alpha}_{i}$-$^{13}C^{\alpha}_{i}$-$^{15}N_{i}$) and to the nitrogen of the adjacent residue *i*+1 ($^{1}H^{\alpha}_{i}$-$^{13}C^{\alpha}_{i}$-$^{15}N_{i+1}$) (Table 1). Because the prolyl residues were the only ones labeled uniformly with ^{13}C and ^{15}N and since P100 and P101 constitute the sole P–P sequence in IscU, P101 is the only residue whose nitrogen yielded two sets of prolyl $^{1}H^{\alpha}$-$^{13}C^{\alpha}$ signals. We were thus able to unambiguously identify signals from P101 from the -$^{1}H^{\alpha}_{P100}$-$^{13}C^{\alpha}_{P100}$-$^{15}N_{P101}$ connectivity (Table 1). Moreover, because the sample contained [^{15}N]-Ala, we assigned signals to P35 from the observed $^{1}H^{\alpha}_{P35}$-$^{13}C^{\alpha}_{P35}$-$^{15}N_{A36}$ connectivity in the 3D HACAN spectrum (Table 1). The remaining $^{1}H^{\alpha}$-$^{13}C^{\alpha}$-^{15}N peak in the spectrum was assigned to P14 ($^{1}H^{\alpha}_{P14}$-$^{13}C^{\alpha}_{P14}$-$^{15}N_{P14}$).

The same strategy was used to assign the proline signals of the D-state, except that the IscU sample contained no Zn^{2+} and data were collected at 45 °C. Although a single set of peaks was observed for P14 in the S-state ($^{1}H^{\alpha}$ 4.226 ppm, $^{13}C^{\alpha}$ 64.79 ppm), two sets of peaks were found corresponding to P14 in the D-state: one with ($^{1}H^{\alpha}$ 4.743 ppm, $^{13}C^{\alpha}$ 62.94 ppm) and the other with ($^{1}H^{\alpha}$ 4.597 ppm, $^{13}C^{\alpha}$ 62.91 ppm). We refer to these two sets of peaks as P14a and P14b, respectively (see Figure 1b). The origin of this local structural heterogeneity remains to be determined.

Prolyl peptide bond configurations from NMR chemical shifts

Previous studies of peptidyl-prolyl *cis-trans* isomerization have shown that prolyl residues with *cis* peptide bonds typically have $^{13}C^{\beta}$ signals around 25 ppm and $^{13}C^{\gamma}$ signals near 35 ppm, with ($\delta^{13}C^{\gamma} - \delta^{13}C^{\beta}$) ≈ 10 ppm; conversely, prolyl residues with *trans* peptide bonds typically have $^{13}C^{\beta}$ signals around 27 ppm and $^{13}C^{\gamma}$ signals near 32 ppm, with ($\delta^{13}C^{\gamma} - \delta^{13}C^{\beta}$) ≈ 5 ppm (28–32). We determined the chemical shifts of the ^{13}C atoms of each prolyl residue from 3D (H)CCH TOCSY spectra (Table 2). When the protein was in the S-state, the chemical shift difference ($\delta^{13}C^{\gamma}$ - $\delta^{13}C^{\beta}$) for all four prolyl residues was ~5 ppm, indicating that they are all *trans* (Figure 2a). However, when the protein was in the D-state, the chemical shift difference was ~5 ppm for P35 and P100, showing that they remain *trans*, but ~10 ppm for P14a, P14b, and P101, indicating that they have become *cis* (Figure 2b).

An algorithm has been developed (implemented in the Promega program) for calculation of the statistical probability of a *trans* or *cis* Xaa–Pro peptide bond from the sequence of the protein and the prolyl chemical shifts and backbone chemical shifts of neighboring residues (31). Analysis of our data by this program confirmed the configurations for the prolyl peptide bonds reported above at normalized likelihood values of greater than or equal to 0.998 (Table 3).

Prolyl peptide bond configurations from nuclear Overhauser effect (NOE) measurements

Another standard way to determine the Xaa–Pro peptide bond configuration is to measure the relative distances between hydrogen atoms on adjacent residues by means of the nuclear Overhauser effect (NOE). In a *trans* peptide bond the H^{α} of the preceding residue is close to the prolyl $H^{\delta 2}$ and $H^{\delta 3}$, whereas in a *cis* peptide bond the H^{α} of the preceding residue is close to the prolyl H^{α} (see Figure S3) The 3D ^{13}C-edited ^{1}H-^{1}H NOESY spectrum of [U-^{13}C, ^{15}N-Pro]-IscU, at 45 °C where the protein is in the D-state, exhibited two NOE signals between P100 and P101 indicative of a *cis* peptide bond (Figure 3a): $H^{\alpha}_{P101}\cdots H^{\alpha}_{P100}$-$C^{\alpha}_{P100}$ and $H^{\alpha}_{P100}\cdots H^{\alpha}_{P101}$-$C^{\alpha}_{P101}$. The same spectrum exhibited an $H^{\alpha}_{N13}\cdots H^{\alpha}_{P14a}$-$C^{\alpha}_{P14a}$ NOE signal between N13 and P14a indicative of a *cis* peptide bond (Figure 3b). Similarly, the $H^{\alpha}_{N13}\cdots H^{\alpha}_{P14b}$-$C^{\alpha}_{P14b}$ NOE signal observed between N13 and P14b confirmed a *cis* peptide bond (Figure 3c). Peak assignments were confirmed by reference to data from 3D H(C)CH TOCSY of [U-^{13}C, ^{15}N-Pro]-IscU and 3D ^{13}C-edited ^{1}H-^{1}H NOESY of [U-^{13}C, ^{15}N]-IscU (Figure 4 and 5). Comparison of ^{13}C-edited ^{1}H-^{1}H NOESY and ^{13}C-filtered, ^{13}C-edited ^{1}H-^{1}H NOESY spectra of IscU in the Zn^{2+}-bound S-state confirmed the presence of $^{1}H^{\alpha}_{i-1}\cdots$prolyl $^{1}H^{\delta}_{i}$ NOEs indicative of *trans* peptide bonds for all four prolyl residues (Figure 6).

Evidence for partial order in the D-state

The 800 MHz ^{1}H-^{15}N HSQC spectrum of [U-^{15}N]-IscU collected at pH 8.0 and 45 °C, where the protein is predominantly in the D-state, exhibited a set of overlapped, non-dispersed peaks and a set of dispersed peaks (Figure 7a). The signals from non-dispersed amide side chains exhibited negative NOEs, whereas the other non-dispersed and dispersed signals exhibited positive NOEs (Figure 7b). We attribute the non-dispersed peaks to residues in disordered regions of the protein and the dispersed peaks to residues in the fold that stabilizes the two *cis* prolyl peptide bonds. Corresponding spectra collected at 70 °C (Figure 7cd) showed only non-dispersed peaks with negative heteronuclear NOE values as expected for a fully unfolded protein.

DISCUSSION

Studies of model peptides have shown that the *trans* configuration of a peptidyl–prolyl peptide bond is favored over the *cis* by about 0.5–1.3 kcal/mol (33). Thus, the energy

required to stabilize two *cis* peptide bonds by at least 95% (to explain the observation of NMR signals from only the *cis* state when IscU is in the D-state) is 4.5 kcal/mol or more; and the stabilization energy may be a major factor in raising the free energy of the D-state so that it is close to that of the S-state. NMR spectra collected at 45 °C, where the protein is predominantly in the D-state (Figure 7ab), show that the protein contains regions of both disorder and order. The protein becomes fully unfolded only at higher temperature (Figure 7cd). These results show that the D-state of IscU is not fully disordered but rather contains an ordered domain that stabilizes two high-energy *cis* peptide bonds.

Thus, IscU can be categorized as a metamorphic protein, one that populates two different conformations of similar free energy that are capable of interconversion under physiological conditions (34). Prior examples of metamorphic proteins, Mad2 (35) and lymphotactin (36, 37), are monomeric in one state and dimeric in the other. By contrast, IscU is monomeric in both states. IscU appears to have evolved to be metamorphic with the two states playing alternate roles in the cycle of iron-sulfur cluster formation and delivery.

Figure 8 illustrates our working model for the steps in Fe-S cluster and assembly, along with schematic representations of states of the peptidyl-prolyl peptide bonds of IscU that change configuration. The D-state, which is the initial substrate for the cysteine desulfurase (17), does not bind metals, leaving the cysteine residues free to accept sulfur to form persulfides. After delivery of iron, the atoms rearrange to form a [2Fe-2S]-cluster ligated by four side chains of IscU in its S-state (3 Cys and 1 His) (19). Product inhibition is minimized because the S-state of IscU binds less strongly to the cysteine desulfurase than the D-state. HscB binds more tightly to the S-state than the D-state (16, 18), which ensures its selective binding to holo-IscU. HscB targets the HscB:holo-IscU complex to the ATP-bound form of the chaperone protein HscA. Following ATP hydrolysis, HscA in its R-state preferentially binds and stabilizes the D-state of IscU (18) leading to irreversible cluster release. Finally, when the ADP bound to HscA is replaced by ATP, HscA reverts to its T-state, and apo-IscU is released (18). The conformational changes of the scaffold protein IscU accompanied by peptidyl-prolyl *cis-trans* isomerizations thus serve to increase the efficiency of iron-sulfur cluster and delivery. Because the free energies of the S- and D-states are similar, very little of the binding energy is required to shift the equilibrium.

Supplementary Material

Refer to Web version on PubMed Central for supplementary material.

Abbreviations used

DSS	4,4-dimethyl-4-silapentane-1-sulfonic acid
EDTA	2,2′,2″,2‴-(ethane-1,2-diyldinitrilo)tetraacetic acid
HSQC	heteronuclear single-quantum correlation
NMR	nuclear magnetic resonance
NOE	nuclear Overhauser enhancement

References

1. Ayala-Castro C, Saini A, Outten FW. Fe-S cluster assembly pathways in bacteria. Microbiol Mol Biol Rev. 2008; 72:110–125. [PubMed: 18322036]
2. Johnson MK. Iron-sulfur proteins: new roles for old clusters. Curr Opin Chem Biol. 1998; 2:173–181. [PubMed: 9667933]

3. Rees DC, Howard JB. The interface between the biological and inorganic worlds: Iron-sulfur metalloclusters. Science. 2003; 300:929–931. [PubMed: 12738849]
4. Campuzano V, Montermini L, Molto MD, Pianese L, Cossee M, Cavalcanti F, Monros E, Rodius F, Duclos F, Monticelli A, Zara F, Canizares J, Koutnikova H, Bidichandani SI, Gellera C, Brice A, Trouillas P, De Michele G, Filla A, De Frutos R, Palau F, Patel PI, Di Donato S, Mandel JL, Cocozza S, Koenig M, Pandolfo M. Friedreich's ataxia: autosomal recessive disease caused by an intronic GAA triplet repeat expansion. Science. 1996; 271:1423–1427. [PubMed: 8596916]
5. Rouault TA, Tong WH. Iron-sulfur cluster biogenesis and human disease. Trends Genet. 2008; 24:398–407. [PubMed: 18606475]
6. Sheftel A, Stehling O, Lill R. Iron-sulfur proteins in health and disease. Trends in Endocrinology & Metabolism. 2010; 21:302–314. [PubMed: 20060739]
7. Shi Y, Ghosh MC, Tong WH, Rouault TA. Human ISD11 is essential for both iron-sulfur cluster assembly and maintenance of normal cellular iron homeostasis. Hum Mol Genet. 2009; 18:3014–3025. [PubMed: 19454487]
8. Kato S, Mihara H, Kurihara T, Takahashi Y, Tokumoto U, Yoshimura T, Esaki N. Cys-328 of IscS and Cys-63 of IscU are the sites of disulfide bridge formation in a covalently bound IscS/IscU complex: implications for the mechanism of iron-sulfur cluster assembly. Proc Natl Acad Sci U S A. 2002; 99:5948–5952. [PubMed: 11972033]
9. Nuth M, Cowan JA. Iron-sulfur cluster biosynthesis: characterization of IscU-IscS complex formation and a structural model for sulfide delivery to the [2Fe-2S] assembly site. J Biol Inorg Chem. 2009; 14:829–839. [PubMed: 19308466]
10. Shi R, Proteau A, Villarroya M, Moukadiri I, Zhang L, Trempe JF, Matte A, Armengod ME, Cygler M. Structural basis for Fe-S cluster assembly and tRNA thiolation mediated by IscS protein-protein interactions. PLoS Biol. 2010; 8:e1000354. [PubMed: 20404999]
11. Zhang W, Urban A, Mihara H, Leimkuhler S, Kurihara T, Esaki N. IscS functions as a primary sulfur-donating enzyme by interacting specifically with MoeB and MoaD in the biosynthesis of molybdopterin in *Escherichia coli*. J Biol Chem. 2010; 285:2302–2308. [PubMed: 19946146]
12. Cupp-Vickery JR, Vickery LE. Crystal structure of Hsc20, a J-type Co-chaperone from *Escherichia coli*. J Mol Biol. 2000; 304:835–845. [PubMed: 11124030]
13. Hoff KG, Ta DT, Tapley TL, Silberg JJ, Vickery LE. Hsc66 substrate specificity is directed toward a discrete region of the iron-sulfur cluster template protein IscU. J Biol Chem. 2002; 277:27353–27359. [PubMed: 11994302]
14. Vickery LE, Cupp-Vickery JR. Molecular chaperones HscA/Ssq1 and HscB/Jac1 and their roles in iron-sulfur protein maturation. Crit Rev Biochem Mol Biol. 2007; 42:95–111. [PubMed: 17453917]
15. Kim JH, Tonelli M, Kim T, Markley JL. Three-Dimensional Structure and Determinants of Stability of the Iron-Sulfur Cluster Scaffold Protein IscU from Escherichia coli. Biochemistry. 2012; 51:5557–5563. [PubMed: 22734684]
16. Kim JH, Füzéry AK, Tonelli M, Ta DT, Westler WM, Vickery LE, Markley JL. Structure and dynamics of the iron-sulfur cluster assembly scaffold protein IscU and its interaction with the cochaperone HscB. Biochemistry. 2009; 48:6062–6071. [PubMed: 19492851]
17. Kim JH, Tonelli M, Markley JL. Disordered form of the scaffold protein IscU is the substrate for iron-sulfur cluster assembly on cysteine desulfurase. Proc Natl Acad Sci U S A. 2012; 109:454–459. [PubMed: 22203963]
18. Kim JH, Tonelli M, Frederick RO, Chow DC, Markley JL. Specialized Hsp70 Chaperone (HscA) Binds Preferentially to the Disordered Form, whereas J-protein (HscB) Binds Preferentially to the Structured Form of the Iron-Sulfur Cluster Scaffold Protein (IscU). J Biol Chem. 2012; 287:31406–31413. [PubMed: 22782893]
19. Shimomura Y, Kamikubo H, Nishi Y, Masako T, Kataoka M, Kobayashi Y, Fukuyama K, Takahashi Y. Characterization and crystallization of an IscU-type scaffold protein with bound [2Fe-2S] cluster from the hyperthermophile, *Aquifex aeolicus*. J Biochem. 2007; 142:577–586. [PubMed: 17846064]
20. Tapley TL, Cupp-Vickery JR, Vickery LE. Structural determinants of HscA peptide-binding specificity. Biochemistry. 2006; 45:8058–8066. [PubMed: 16800630]

21. Dutkiewicz R, Schilke B, Cheng S, Knieszner H, Craig EA, Marszalek J. Sequence-specific interaction between mitochondrial Fe-S scaffold protein Isu and Hsp70 Ssq1 is essential for their in vivo function. J Biol Chem. 2004; 279:29167–29174. [PubMed: 15123690]
22. Hoff KG, Silberg JJ, Vickery LE. Interaction of the iron-sulfur cluster assembly protein IscU with the Hsc66/Hsc20 molecular chaperone system of *Escherichia coli*. Proc Natl Acad Sci USA. 2000; 97:7790–7795. [PubMed: 10869428]
23. Cheng H, Westler WM, Xia B, Oh BH, Markley JL. Protein expression, selective isotopic labeling, and analysis of hyperfine-shifted NMR signals of *Anabaena* 7120 vegetative [2Fe-2S] ferredoxin. Arch Biochem Biophys. 1995; 316:619–634. [PubMed: 7840674]
24. Füzéry AK, Tonelli M, Ta DT, Cornilescu G, Vickery LE, Markley JL. Solution structure of the iron-sulfur cluster cochaperone HscB and its binding surface for the iron-sulfur assembly scaffold protein IscU. Biochemistry. 2008; 47:9394–9404. [PubMed: 18702525]
25. Delaglio F, Grzesiek S, Vuister GW, Zhu G, Pfeifer J, Bax A. NMRPIPE - A Multidimensional Spectral Processing System Based on UNIX Pipes. J Biomol NMR. 1995; 6:277–293. [PubMed: 8520220]
26. Goddard, TD.; Kneller, DG. Sparky. Vol. 3. University of California; San Francisco, San Francisco:
27. Kanelis V, Donaldson L, Muhandiram DR, Rotin D, Forman-Kay JD, Kay LE. Sequential assignment of proline-rich regions in proteins: application to modular binding domain complexes. J Biomol NMR. 2000; 16:253–259. [PubMed: 10805132]
28. Dorman DE, Torchia DA, Bovey FA. Carbon-13 and proton nuclear magnetic resonance observations of the conformation of poly(L-proline) in aqueous salt solutions. Macromolecules. 1973; 6:80–82. [PubMed: 4778412]
29. Howarth OW, Lilley DMJ. Carbon-13-NMR of Peptides and Proteins. Prog Nucl Mag Res Sp. 1978; 12:1–40.
30. Schubert M, Labudde D, Oschkinat H, Schmieder P. A software tool for the prediction of Xaa-Pro peptide bond conformations in proteins based on 13C chemical shift statistics. J Biomol NMR. 2002; 24:149–154. [PubMed: 12495031]
31. Shen Y, Bax A. Prediction of Xaa-Pro peptide bond conformation from sequence and chemical shifts. J Biomol NMR. 2010; 46:199–204. [PubMed: 20041279]
32. Siemion IZ, Wieland T, Pook KH. Influence of the distance of the proline carbonyl from the β and γ carbon on the ^{13}C chemical shifts. Angew Chem Int Ed Engl. 1975; 14:702–703. [PubMed: 812384]
33. Grathwohl C, Wüthrich K. NMR Studies of the Rates of Proline cis - trans Isomerization in Oligopeptides. Biopolymers. 1981; 20:2623–2633.
34. Murzin AG. Biochemistry - Metamorphic proteins. Science. 2008; 320:1725–1726. [PubMed: 18583598]
35. Mapelli M, Massimiliano L, Santaguida S, Musacchio A. The Mad2 conformational dimer: structure and implications for the spindle assembly checkpoint. Cell. 2007; 131:730–743. [PubMed: 18022367]
36. Kuloglu ES, McCaslin DR, Markley JL, Volkman BF. Structural rearrangement of human lymphotactin, a C chemokine, under physiological solution conditions. J Biol Chem. 2002; 277:17863–17870. [PubMed: 11889129]
37. Tyler RC, Murray NJ, Peterson FC, Volkman BF. Native-state interconversion of a metamorphic protein requires global unfolding. Biochemistry. 2011; 50:7077–7079. [PubMed: 21776971]

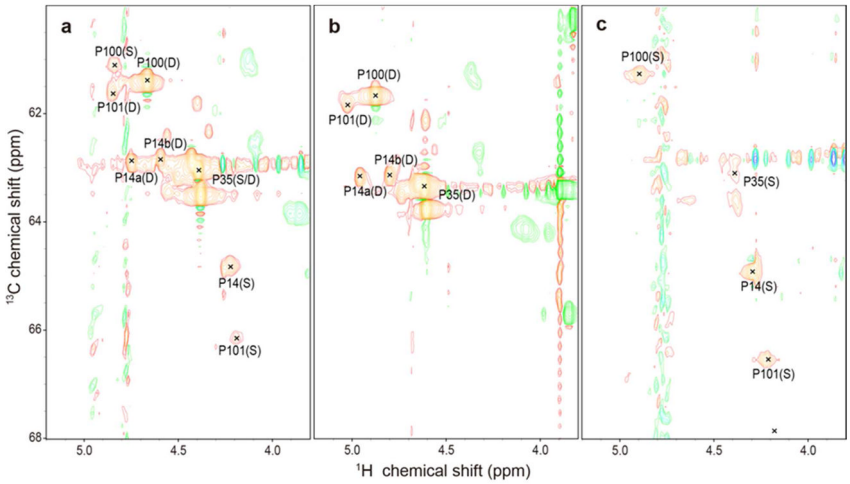

Figure 1.

Aliphatic regions of 2D ^{1}H-^{13}C HSQC spectra of 1 mM [U-^{13}C, ^{15}N-Pro]-IscU acquired at 600 MHz (^{1}H) under the conditions specified. (a) Spectrum of apo-IscU acquired at pH 8.0 and 25 °C, where the protein is a mixture of the S- and D-states. (b) Spectrum of apo-IscU acquired at 45 °C, where the protein is in the D-state. (c) Spectrum of the Zn-bound form of IscU acquired at pH 8.0 and 25 °C, where the protein is in the S-state. Assignments to individual prolyl residues were determined as described in the text. Each NMR sample in a and c contained 1 mM [U-^{13}C, ^{15}N-Pro]-IscU, 50 mM Tris-HCl (pH 8.0), 0.5 mM EDTA, 5 mM DTT, 150 mM NaCl, 50 μM DSS, and 50 μM NaN_3 in 10% D_2O. The NMR sample in b contained 1 mM [U-^{13}C, ^{15}N-Pro]-IscU:Zn^{2+}, 50 mM Tris-HCl (pH 8.0), 5 mM DTT, 150 mM NaCl, 50 μM DSS, and 50 μM NaN_3 in 10% D_2O. The same data at a lower contour is shown in Figure S1.

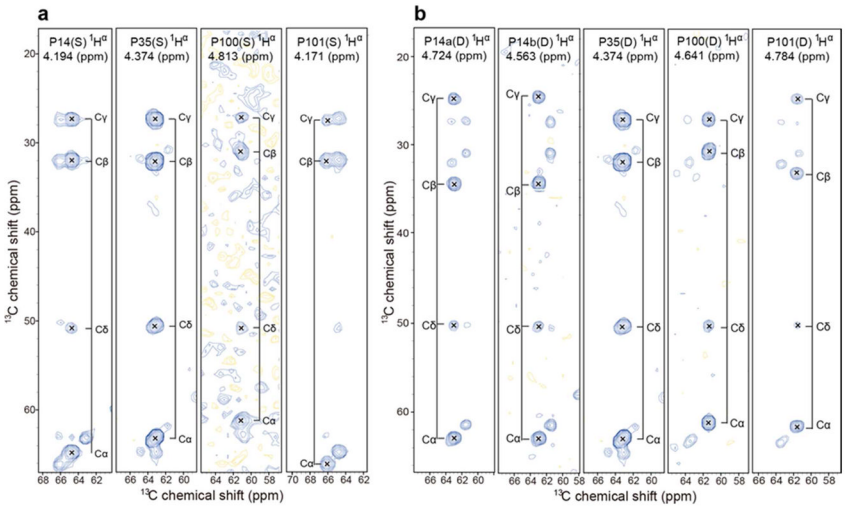

Figure 2.

2D strip plots from 3D (H)CCH-TOCSY spectra of IscU acquired at 600 MHz (^{1}H). The NMR sample contained 1 mM [U-^{13}C, ^{15}N-Pro]-IscU, 50 mM Tris-HCl (pH 8.0), 5 mM DTT, 150 mM NaCl, 50 μM DSS, and 50 μM NaN_3 in 10% D_2O. 2D strips were taken at the chemical shifts of the prolyl $^1H^\alpha$, shown at the top of each strip. (a) Spectrum of the S-state of IscU stabilized as the Zn^{2+} complex at 25 °C. (b) Spectra of the D-state of IscU acquired at 45°C.

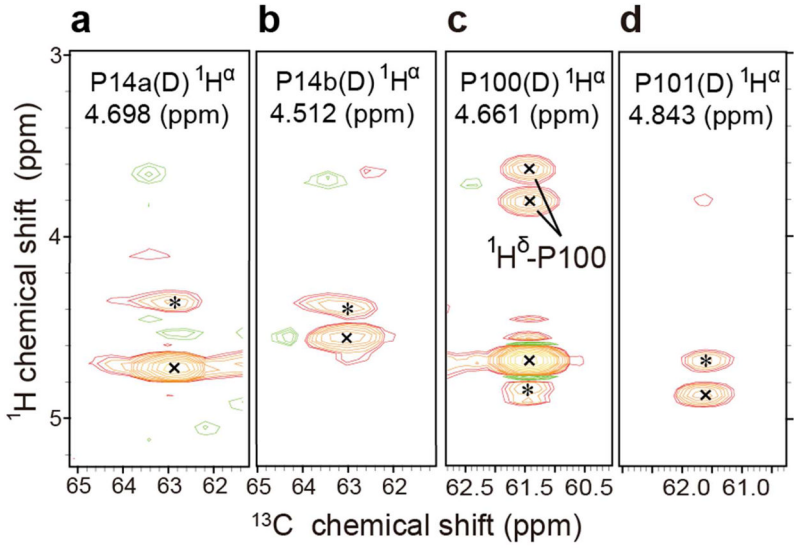

Figure 3.

3D ^{13}C-edited 900 MHz (^{1}H) NOESY data acquired at 45 °C at a mixing time of 125 ms, which confirm that the P100-P101 and N13-P14 peptide bonds of IscU are *cis* in the D-state. The sample contained 1 mM [U-^{13}C, ^{15}N-Pro]-IscU, 50 mM Tris-HCl (pH 8.0), 0.5 mM EDTA, 5 mM DTT, 150 mM NaCl, 50 μM DSS, and 50 μM NaN_3 in 10% D_2O. Peaks labeled "x" are diagonal peaks; peaks labeled "*" are NOE peaks. (a) 2D strip at the $^1H^\alpha$ chemical shift of P14a; the NOE peak is from (N13)$^1H^\alpha$···$^1H^\alpha$-$^{13}C^\alpha$(P14a). (b) 2D strip at the $^1H^\alpha$ chemical shift of P14b; the NOE peak is from (N13)$^1H^\alpha$···$^1H^\alpha$-$^{13}C^\alpha$(P14b). (c) 2D strip at the $^1H^\alpha$ chemical shift of P100; the NOE peak is from (P101)$^1H^\alpha$···$^1H^\alpha$-$^{13}C^\alpha$(P100). The peaks at ^{1}H chemical shifts of 3.6 ppm and 3.8 ppm arise from NOEs from (P100)$^1H^\alpha$ to the $^1H^{\delta 2}$ and $^1H^{\delta 3}$ of P100 and/or P101. (d) 2D strip at the $^1H^\alpha$ chemical shift of P101; the NOE peak is from (P100)$^1H^\alpha$···$^1H^\alpha$-$^{13}C^\alpha$(P101).

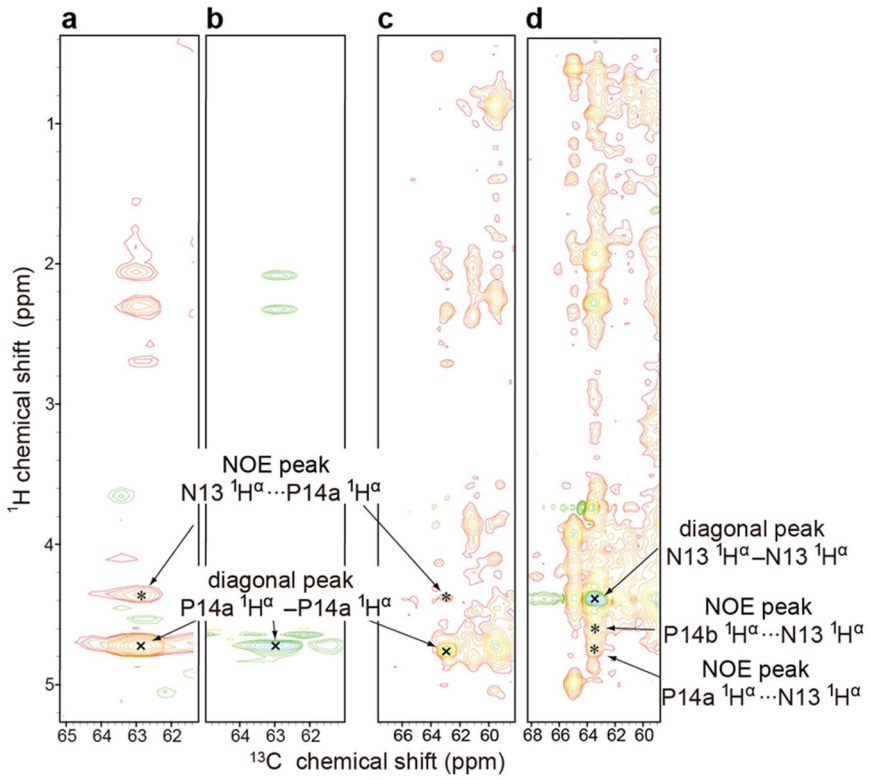

Figure 4.

NMR spectra collected at 900 MHz (^{1}H) at 45 °C where the protein is in the D-state. The NMR samples contained 1 mM protein, 50 mM Tris-HCl (pH 8.0), 0.5 mM EDTA, 5 mM DTT, 150 mM NaCl, 50 μM DSS, and 50 μM NaN_3 in 10% D_2O. Diagonal peaks are marked by "x" and NOE peaks by "*". (**a**) Strip at the P14a ^{1}H$^\alpha$ chemical shift from a 3D ^{13}C-edited ^{1}H-^{1}H NOESY spectrum (mixing time 125 ms) of [U-^{13}C,^{15}N-Pro]-IscU. (**b**) Strip at the P14a ^{1}H$^\alpha$ chemical shift from a 3D H(C)CH-TOCSY spectrum of [U-^{13}C, ^{15}N-Pro]-IscU. The cross peak matches the ^{1}H$^\alpha$-^{13}C$^\alpha$ position of the diagonal in panel A. (**c**) Strip at the P14a ^{1}H$^\alpha$ chemical shift from a 3D ^{13}C-edited ^{1}H-^{1}H NOESY spectrum (mixing time 125 ms) of [U-^{13}C,^{15}N]-IscU. The uniformly labeled sample exhibits cross peaks at the same positions as those from the selectively labeled sample (panel A). (**d**) Strip at the N13 ^{1}H$^\alpha$ chemical shift from a 3D ^{13}C-edited ^{1}H-^{1}H NOESY spectrum (mixing time 125 ms) of [U-^{13}C, ^{15}N]-IscU. Both P14a ^{1}H$^\alpha$ and P14b ^{1}H$^\alpha$ exhibit NOEs with N13 ^{1}H$^\alpha$.

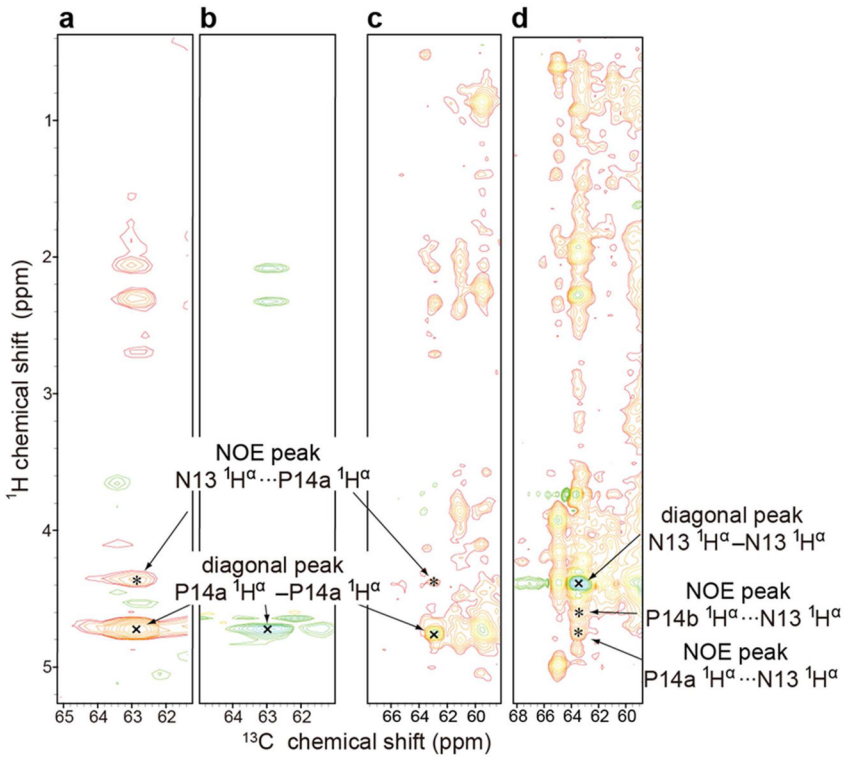

Figure 5.

NMR spectra collected at 900 MHz (^{1}H) at 45 °C where the protein is in the D-state. The NMR samples contained 1 mM protein, 50 mM Tris-HCl (pH 8.0), 0.5 mM EDTA, 5 mM DTT, 150 mM NaCl, 50 μM DSS, and 50 μM NaN_3 in 10% D_2O. Diagonal peaks are marked by "x" and NOE peaks by "*". (**a**) Strip at the P14b ^{1}H$^\alpha$ chemical shift from a 3D ^{13}C-edited ^{1}H-^{1}H NOESY spectrum (mixing time 125 ms) of [U-^{13}C, ^{15}N-Pro]-IscU. (**b**) Strip at the P14b ^{1}H$^\alpha$ chemical shift from a 3D H(C)CH-TOCSY spectrum of [U-^{13}C, ^{15}N-Pro]-IscU. The cross peak matches the ^{1}H$^\alpha$-^{13}C$^\alpha$ position of the diagonal in panel A. (**c**) Strip at the P14b ^{1}H$^\alpha$ chemical shift from a 3D ^{13}C-edited ^{1}H-^{1}H NOESY spectrum (mixing time 125 ms) of [U-^{13}C,^{15}N]-IscU. The uniformly labeled sample exhibits cross peaks at the same positions as those from the selectively labeled sample (panel A). (**d**) Same spectrum as panel **d** in Figure S2. Strip at the N13 ^{1}H$^\alpha$ chemical shift from a 3D ^{13}C-edited ^{1}H-^{1}H NOESY spectrum of [U-^{13}C, ^{15}N]-IscU. Both P14a ^{1}H$^\alpha$ and P14b ^{1}H$^\alpha$ exhibit NOEs with N13 ^{1}H$^\alpha$.

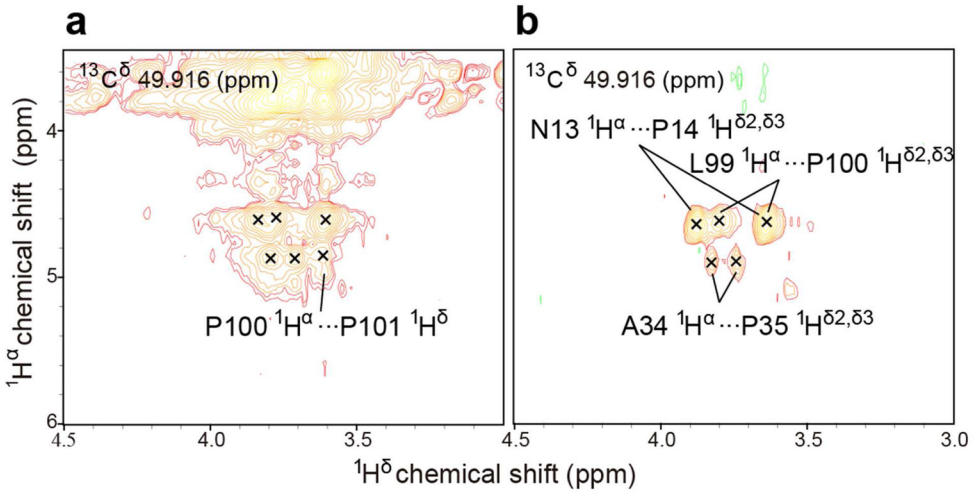

Figure 6.

900 MHz (^{1}H) spectra of [U-^{13}C, ^{15}N-Pro]-IscU at 25 °C in the presence of Zn^{2+} where the protein is in the S-state. The NMR sample contained, 1 mM protein,1 mM $ZnCl_2$, 50 mM Tris-HCl (pH 8.0), 5 mM DTT, 150 mM NaCl, 50 μMDSS, and 50 μM NaN_3 in 10% D_2O,. (**a**) 2D strip from a 3D ^{13}C-edited ^{1}H-^{1}H NOESY spectrum without filtration(125 ms mixing time). (**b**) 3D ^{13}C-filtered/^{13}C-edited ^{1}H-^{1}H NOESY spectrum (mixing time 125 ms) showing only NOE cross-peaks between protons attached to carbon-13 and protons attached to carbon-12 ($^{13}C^{\delta}$–H^{δ}···H^{α}–$^{12}C^{\alpha}$ NOEs survive; $^{13}C^{\delta}$–H^{δ}···H^{α}–$^{13}C^{\alpha}$ NOEs, such as those within the same or between the two prolyl residues, are filtered out). $^{1}H^{\delta2/\delta3}$...$^{1}H^{\alpha}$ NOE signals from residue pairs N13-P14, A34-P35, and L99-P100 (panel **b**) confirm that these peptide bonds are *trans*. The same peaks are observed in the unfiltered spectrum (panel **a**). Panel **a** contains an additional resolved $^{1}H^{\delta}$...$^{1}H^{\alpha}$ NOE peak assigned to the P100-P101 residue pair, which confirms that the peptide bond is *trans*.

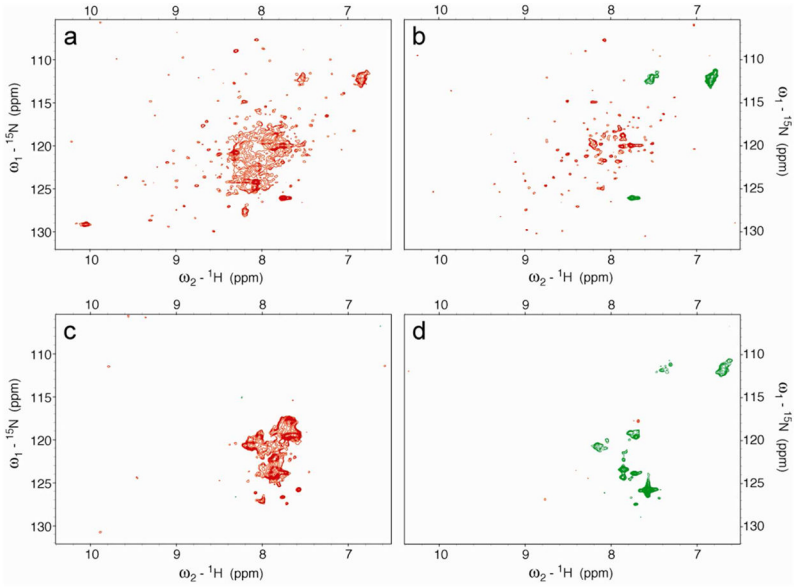

Figure 7.

800 MHz ^{1}H-^{15}N HSQC spectra of [U-^{15}N]-IscU at pH 8.0 and at different temperatures with positive peaks in orange and negative peaks in green. (**a**) 45 °C without NOE. (**b**) 45 °C with NOE;. (**c**) 70 °C without NOE. (**d**) 70 °C with NOE.

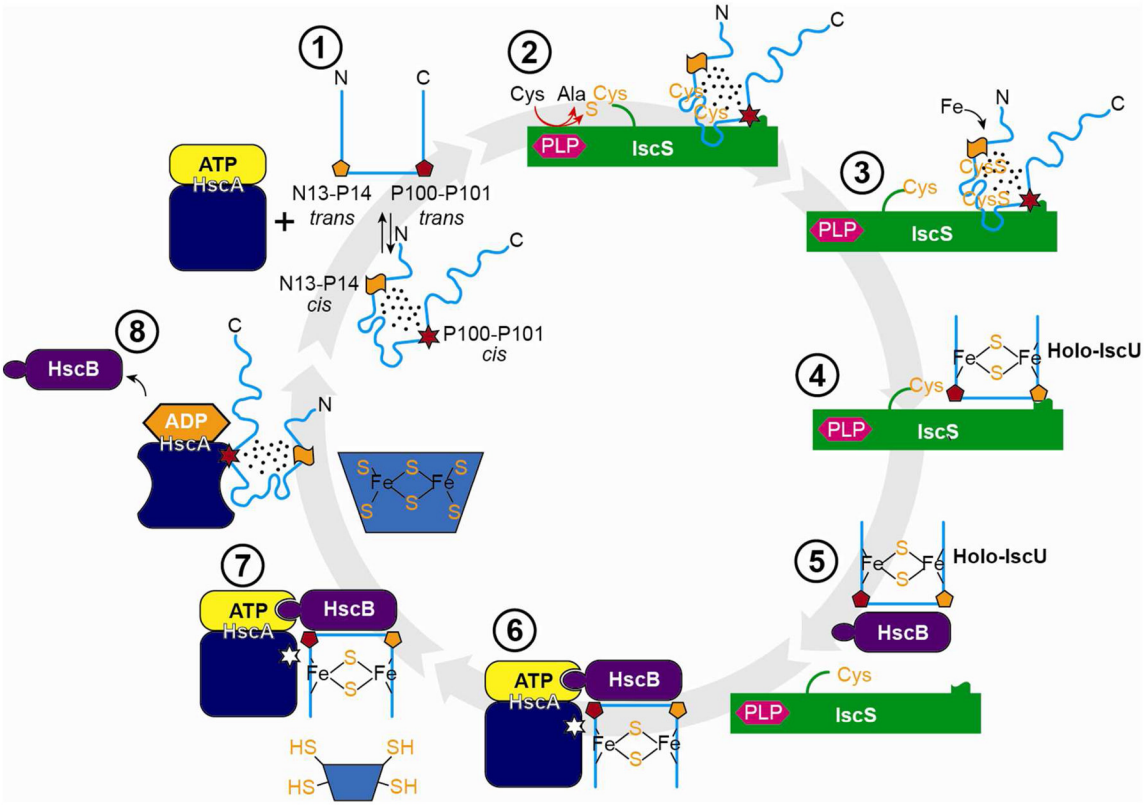

Figure 8.

Working model for the mechanism of iron-sulfur cluster assembly and transfer. (1) Free IscU in DS equilibrium. (2) Complex between the cysteine desulfurase (IscS) and the D-form of IscU. (3) Addition of sulfur to Cys residues of IscU. (4) Addition of iron to form a [2Fe-2S] cluster stabilized by the S-state of IscU. (5) Transfer of holo-IscU to the co-chaperone (HscB). (6) Docking of holo-IscU to the HscA-ATP complex. (7) Approach of an acceptor apo-protein. (8) Transfer of the Fe-S cluster to the acceptor protein, release of HscB, and binding of the D-state of IscU to HscA-ADP. (1) Return to the starting state by exchange of HscA-bound ADP by ATP and release of IscU.

Table 1

Signals Observed in the 3D HACAN Spectrum of ([U-^{13}C,^{15}N]-Pro, [^{15}N]-Ala)-IscU:Zn^{2+} that Led to Assignment of Signals to the Four Prolyl Residues in the S-State.

Residue[a]	^{15}N signals visible from $^{1}H^{\alpha}/^{13}C^{\alpha}$	$^{1}H^{\alpha}/^{13}C^{\alpha}$ signals visible from ^{15}N
Pro14	$H^{\alpha}{}_{P14}$-$C^{\alpha}{}_{P14}$-N_{P14}	$H^{\alpha}{}_{P14}$-$C^{\alpha}{}_{P14}$-N_{P14}
Pro35	$H^{\alpha}{}_{P35}$-$C^{\alpha}{}_{P35}$-N_{P35} $H^{\alpha}{}_{P35}$-$C^{\alpha}{}_{P35}$-N_{A36}	$H^{\alpha}{}_{P35}$-$C^{\alpha}{}_{P35}$-N_{P35}
Ala36	None	$H^{\alpha}{}_{P35}$-$C^{\alpha}{}_{P35}$-N_{A36}
Pro100	$H^{\alpha}{}_{P100}$-$C^{\alpha}{}_{P100}$-N_{P100} $H^{\alpha}{}_{P100}$-$C^{\alpha}{}_{P100}$-N_{P101}	$H^{\alpha}{}_{P100}$-$C^{\alpha}{}_{P100}$-N_{P101}
Pro101	$H^{\alpha}{}_{P101}$-$C^{\alpha}{}_{P101}$-N_{P101}	$H^{\alpha}{}_{P100}$-$C^{\alpha}{}_{P100}$-N_{P101} $H^{\alpha}{}_{P101}$-$C^{\alpha}{}_{P101}$-N_{P101}

[a]The strict conservation of these residues is illustrated in Figure S1.

Table 2

NMR Assignments for the Prolyl Residues of the S-and D-States of IscU

IscU state	Residue	Chemical shift (ppm)				$\delta^{13}C^{\beta} - \delta^{13}C^{\gamma}$ (ppm)	Peptide bond configuration
		$^{13}C^{\alpha}$	$^{1}H^{\alpha}$	$^{13}C^{\beta}$	$^{13}C^{\gamma}$		
Structured state (S)[a]	Pro14	64.79	4.226	31.98	27.35	4.63	*trans*
	Pro35	63.06	4.410	32.05	27.40	4.65	*trans*
	Pro100	61.16	4.845	30.91	27.08	3.83	*trans*
	Pro101	66.13	4.204	32.03	27.45	4.58	*trans*
Disordered state (D)[b]	Pro14a	62.95	4.743	34.45	24.82	9.63	*cis*
	Pro14b	62.91	4.597	34.34	24.73	9.61	*cis*
	Pro35	63.06	4.410	32.05	27.40	4.65	*trans*
	Pro100	61.36	4.667	30.88	27.36	3.52	*trans*
	Pro101	61.50	4.848	33.07	24.74	8.33	*cis*

Table 3

Predictions of *cis* Xaa-Pro Likelihood for *E. coli* IscU by the Promega Server (31) from Amino Acid Sequence and Chemical Shift Data.

State	Residue	Likelihood for Pro to be *cis*	Normalized likelihood for Pro to be *cis*
Structured state (S)	Pro14	0.000	0.000
	Pro35	0.000	0.000
	Pro100	0.000	0.000
	Pro101	0.000	0.000
Disordered state (D)	Pro14a	1.000	0.998
	Pro14b	1.000	0.998
	Pro35	0.001	0.000
	Pro100	0.001	0.000
	Pro101	0.999	0.988